17th World Conference on Earthquake Engineering, 17WCEE
Sendai, Japan - September 13th to 18th 2020

SEISMIC FRAGILITY ANALYSIS OF A HIGH-RISE CONCRETE-WOOD HYBRID STRUCTURAL SYSTEM

Haibei Xiong [(1)], Jiawei Chen [(2)], Carlos Ventura[(3)]

[(1)] *Professor, Tongji University, xionghaibei@tongji.edu.cn*
[(2)] *Ph.D. student, Tongji University, jiawei_chen@tongji.edu.cn*
[(3)] *Professor, University of British Columbia, Canada, ventura@civil.ubc.ca*

Abstract

Focusing on the construction of tall wood buildings in dense urban cities, an innovative concrete-wood hybrid structural system has been proposed and studied since 2016. Such hybrid system is mainly composed of two parts: a concrete frame-tube structure with slabs at every third story as the main structure for lateral resistance and stiffness, and several prefabricated 3-story-high timber modules setting on every concrete slab as the substructures for self-resistance. Between the two parts, either bolt connection or rubber bearing connection is adopted for transmitting the force and displacement. In this paper, a performance-based seismic fragility analysis of the hybrid system was presented. Firstly, three performance levels of this hybrid system were established, including immediate occupancy (IO) level, life safety (LS) level, and collapse prevention (CP) level, and the performance criteria for different seismic hazard levels were determined. Then, incremental dynamic analysis utilizing OpenSees was conducted to obtain the seismic response of the hybrid system. Twenty-four motion records, including twelve near-field earthquake motions and twelve far-field motions, were used for the analysis, which were all scaled to the design response spectrum with spectral acceleration amplitude from 0.05g to 2.10g in twenty-one seismic levels. Taking drift responses of both concrete structure and wood substructures and displacement response of rubber bearing connection as performance criteria, performance curves were established by considering different target non-exceedance probabilities. Based on the performance curves, seismic fragility analysis of the hybrid system was carried out, and the results showed that: (1) The hybrid system was more sensitive to far-field earthquakes, as the exceedance probability (EP) of the whole hybrid system with bolt connection, and the main concrete structure with rubber bearing connection under far-field earthquakes was larger than those under near-field earthquakes, while the EP of rubber bearing connection and wood substructures with rubber bearings were similar. (2) The failure sequence of the hybrid system under both near-field and far-field earthquakes was satisfactory. In the CP level, the failure probability of concrete main structure was obviously smaller than that of wood substructures in the hybrid system with bolt connection, while in the system adopting rubber bearing connection, the isolation layer would firstly achieve the target performance level, then the wood substructures, and finally the concrete main structure. (3) The rubber bearing connection had a dominant isolation effect on the wood substructures and a seismic reduction effect on the concrete main structure, as the EP of wood substructures with rubber bearing connection was much smaller than that with bolt connection in all three levels. While, for the concrete main structure, the EP of that with rubber bearing connection was evidently smaller than that with bolt connection in the CP level, but it was similar in the IO and LS levels under either near-field earthquakes or far-field earthquakes. This study provides performance-based seismic evaluations on the concrete-wood hybrid structural system, which supports the future applications of such hybrid systems in high-rise buildings.

Keywords: concrete-wood hybrid structure, seismic fragility analysis, incremental dynamic analysis, seismic performance levels, OpenSees

1. Introduction

With the increasing urban density and the promotion of more sustainable construction materials and building alternatives, growing attempts have been made to develop tall wood or wood-hybrid buildings worldwide. Feasibility studies for novel high-rise wood-based hybrid structural systems were carried out[1,2], and many prototype buildings were tested[3–5]. Meanwhile, several tall wood or wood-hybrid buildings, e.g., the 18-story Brock Commons in Vancouver[6] and the 18-story Mjøstårnet in Brumunddal[7], have been successfully built and are operating well, which shows the high competitiveness of tall wood or wood-hybrid buildings in the aspects of structural performance, environmental friendliness, and construction speed.

Xiong et al.[8] proposed a novel high-rise concrete-wood hybrid structural system in 2016, which is called “Frame and Boxes” (FaB). As shown in Fig.1, such hybrid system is mainly composed of two parts: a concrete frame-tube structure with slabs at every third story as the main structure for lateral resistance and stiffness, and several prefabricated 3-story-high timber modules setting on every concrete slab as the substructures for self-resistance. Characteristics such as integrated structure system, flexible building function, prefabricated construction work and sustainable building materials can be realized by the proposed hybrid system[9]. Numerical studies with response spectrum method or dynamic time-history analysis revealed the feasibility and the great seismic performance of FaB[10], and presented the influence of the connections between the concrete main structure and wood substructures to the whole system[11]. However, more studies are needed to evaluate the seismic performance of such concrete-wood hybrid system under different seismic levels and thus to provide performance-based seismic evaluations before its practical applications.

The performance-based or reliability-based seismic design method has been more and more popular in the field of structural design since it allows structures to be designed for specific target performance objectives. More importantly, this method provides a reasonable approach for the innovative structural systems since the performance of these newly developed systems is not fully understood because of the lack of enough test data or in-field performance history. Rosowsky and Ellingwood[12] proposed a review of performance-based design models and tools, and a procedure for evaluating the response of light wood frame construction under various levels of hazards was also presented. Kim and Rosowsky[13] introduced the fragility techniques for the seismic design of engineered wood-frame shear walls. Li and He[14] conducted a performance-based analysis on the seismic performance of a novel timber-steel hybrid shear wall systems and developed the design procedure for the timber-steel hybrid system. Zhang and Tannert[15] studied the failure probability of a novel tall timber-steel hybrid system FFTT by conducting the seismic reliability analysis with genetic algorithms and analysis of variance with response surface method.

In FaB, the wood substructures are set on the concrete floors and are subjected to floor excitation under earthquakes. The floor excitation tends to be long-duration with long-period spectrum, and the wood substructures are more likely to collapse due to these effects of floor excitation[16]. The seismic fragility analysis for the FaB is thus important. However, few research studies have been reported on the seismic performance of high-rise concrete-wood hybrid structural systems utilizing reliability-based methods or seismic fragility analysis. In this paper, a performance-based seismic fragility analysis for the concrete-wood hybrid system FaB was presented. Three performance levels were firstly established and the performance criteria for different seismic hazard levels were determined. Based on the seismic fragility analysis results, the seismic performance of FaB under near-field and far-field earthquakes with either bolt connection or rubber bearing between the concrete main structure and wood substructures was studied. Meanwhile, the failure sequence of the hybrid system under different levels of earthquakes was discussed.

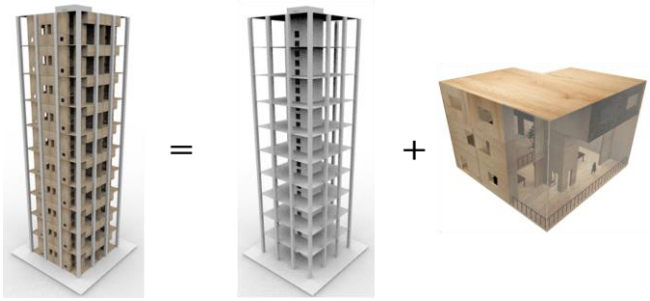

Concrete-wood (Hybrid structure) | Concrete frame-tube (Main structure, Frame) | Timber modules (Substructure, Box)

Fig. 1 – Innovative concrete-wood hybrid structural system FaB

2. Performance-based seismic fragility analysis for FaB

2.1 Numerical models of FaB

Proposed in the preliminary study[11], a reference structure, a typical 30-story office building in Shanghai, which is originally a concrete frame-tube structure, was redesigned using the concrete-wood hybrid structural system. The typical story height of the building is 2.9m, and the height between concrete slabs is 9.4m. The total height of the building is 94m, and the plane size of the building is 24m×24m. Fig.2(a) shows a typical plane of the concrete floor. The concrete slab is the base for the three-story timber modules above. The prefabricated timber modules, which are the light wood construction in this paper, comprised the main functional space of the building. Fig.2(b) shows a typical plane of the wood floor. Other structural details were referred to [11].

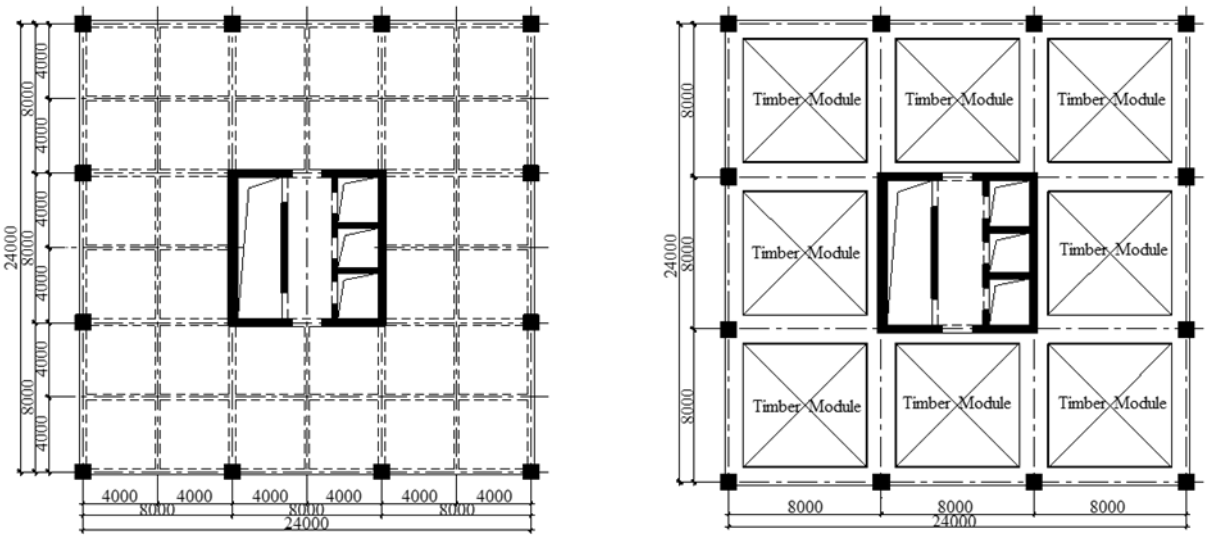

(a) Layout of concrete frame-tube structure (b) Layout of timber modules

Fig.2 – Plane layout of the hybrid structure

Finite element models for FaB were developed utilizing OpenSees[17]. Similar to previous research, the concrete columns and beams were modeled by the displacement-based beam-column element with the fiber section, as shown in Fig.3 (a). The equivalent frame method was adopted to simulate the shear walls, which simplified the planar shear wall to an assembly of 3D frame elements with equivalent lateral resistance behavior[18]. For timber modules, a simplified model[19] was adopted to model the shear walls and floors, in which the lateral performance of the timber shear walls was simulated by diagonal springs with the calibration of the deformation-equivalent stiffness curves and equations, as illustrated in Fig.3 (b).

In this paper, either bolt connection or rubber bearing connection was adopted to connect the wood substructures and concrete main structure; the former was used for a fixed boundary while the latter was used for isolation layers. The Pinching4 model was adopted to calibrate the force-displacement relationship of the bolt connection (Fig.3 (c)), which was based on the results of single-bolted wood-concrete connection tests. The rubber bearings (Fig.3 (d)) were modeled using elastomeric bearing (Bouc-Wen) element with initial elastic stiffness, yield force, and post-yield stiffness ratio setting as 2042N/mm, 12000N and 0.1, respectively. For more modeling details, the reader is kindly referred to the previous study[11].

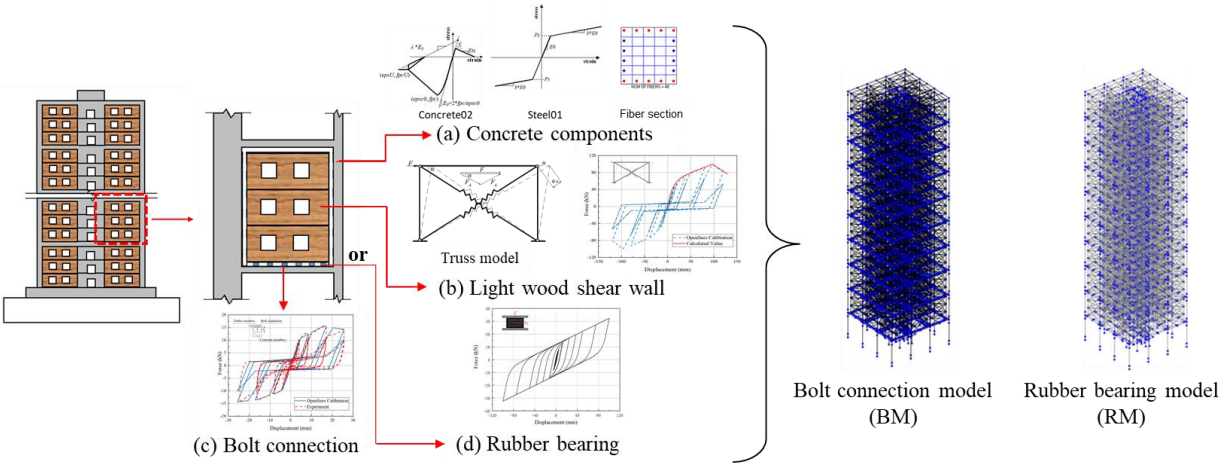

Fig.3 – Finite element models of the hybrid structure

2.2 Fragility analysis

Seismic fragility $F_{C_\theta|D_\theta}$ describes the conditional probability of reaching or exceeding a specified deterministic or random performance level with an intensity measure d_θ, which is defined as

$$F_{C_\theta|D_\theta}=P[C_\theta \geq C_\theta^{PL}|D_\theta = d_\theta] \tag{1}$$

where C_θ describes the state of the structure, C_θ^{PL} is the ultimate state, D_θ is the index of intensity.

In FaB, the concrete main structure, wood substructures and isolation layers show different damage states under earthquakes, and it is difficult to evaluate the overall damage state of the whole hybrid system merely based on the damage state of the concrete structure, wood structures or connections alone. In this paper, it was assumed that the concrete structure, wood structures and connections were in series. In this way, the damage state of the whole hybrid system was represented by the most severe damage state of the three parts of FaB.

The performance-based fragility analysis was conducted in this paper, which considered uncertainties of both structure and seismic input. Fig.4 shows the flowchart of this method. Incremental dynamic analysis (IDA), a widely used method in earthquake engineering, was adopted in the analysis, which utilizes ground motion records with multiple levels of intensity to do the dynamic time-history analysis for a structure model and thus to produce curves of response parameterized versus intensity level[20].

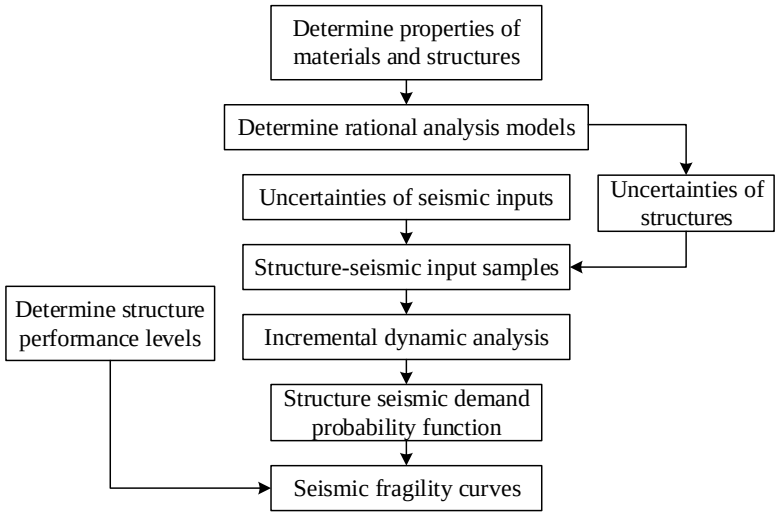

Fig.4 –Flowchart of the performance-based fragility analysis

The seismic fragility curve represents the probability of engineering demand parameters (*EDP*) of a structure exceeding a specified deterministic or random performance level *y* under specified intensity measures (*IM*) (*IM*=*im*), i.e., *P*=(*EDP*>*y*|IM=*im*). The *EDP* of the structure is obeying logical normal distribution, and thus the equation (2) was used to calculate the exceedance probability of the structure under specified earthquake intensity level *IM*.

$$P(u > y \mid IM = im) = 1 - \Phi\left(\frac{\ln y - \overline{\mu}_{\ln u|PGA}}{\overline{\sigma}_{\ln u|PGA}}\right) \tag{2}$$

where $\overline{\mu}_{\ln u|PGA}$ and $\overline{\sigma}_{\ln u|PGA}$ is the logarithmic mean and logarithmic standard deviation of engineering demand parameters under intensity measures equal to *PGA*, $\Phi(g)$ is the standard normal distribution function.

2.3 Seismic input and performance objectives

Three limit states are defined as immediate occupancy (IO), life safety (LS) and collapse prevention (CP) limit states for FaB, and the 50-year exceedance probabilities for the earthquakes considered in the IO, LS and CP limit states are 63%, 10% and 2%, in accordance with the average return period of 50, 475, and 2475 years, respectively. In order to evaluate the seismic performance of FaB under seismic prone zones, 24 records including 12 near-field earthquake motions and 12 far-field motions were selected from the PEER NGA database[21], which are listed in Table 1 and Table 2. These ground motion records were selected and scaled by a response spectrum approach, i.e., the 5% damped spectral value over the plateau region (0.1 - 0.9s) match the spectral acceleration specified in Chinese Code for Seismic Design of Building, as shown in Fig.5.

In order to conduct the incremental dynamic analysis, nonlinear time history analyses were performed at 21 different seismic spectral acceleration levels (i.e., 0.05g, 0.10g, 0.13g, 0.15g, 0.18g, 0.20g, 0.30g, 0.40g, 0.45g, 0.50g, 0.60g, 0.75g, 0.90g, 1.05g, 1.20g, 1.35g, 1.50g, 1.65g, 1.80g, 1.95g and 2.10g), and the ground motion records were scaled to these values, respectively.

Deformation limit state was utilized as the performance criterion for the hybrid system since it was related to both structural and non-structural damage and widely used. All the performance criteria values for the concrete structure, wood substructures and rubber bearing connection under different performance levels are listed in Table 3.

Table 1 – Near-field ground motion records

No.	Name	Station	Year	Fault distance (km)	Magnitude	Duration(s)
1	Imperial Valley-06	El Centro #3	1979	12.85	6.53	39.62
2	Imperial Valley-07	El Centro #2	1979	18.78	5.01	10.86
3	Imperial Valley-07	El Centro #3	1979	16.25	5.01	11.03
4	Superstition Hills-01	Imperial Valley	1987	17.59	6.22	29.85
5	Tottori_Japan	SMN002	2000	16.61	6.61	240.24
6	Tottori_Japan	TTR008	2000	6.88	6.61	299.98
7	Parkfield-02_CA	Cholame 2WA	2004	3.01	6.00	21.08
8	Parkfield-02_CA	Fault Zone 1	2004	2.51	6.00	20.98
9	Darfield_NZ	Botanical Gardens	2010	18.05	7.00	150.00
10	Darfield_NZ	Resthaven	2010	19.48	7.00	150.00
11	Christchurch_NZ	Botanical Gardens	2011	5.55	6.2	45.00
12	Christchurch_NZ	Resthaven	2011	5.13	6.2	50.00

Table 2 – Far-field ground motion records

No.	Name	Station	Year	Fault distance (km)	Magnitude	Duration (s)
1	Chi-Chi_Taiwan	CHY078	1999	77.20	7.62	90.00
2	Chi-Chi_Taiwan	CHY107	1999	50.61	7.62	150.00
3	Chuetsu-oki_Japan	MYG006	2007	226.61	6.80	204.00
4	Chuetsu-oki_Japan	SIT008	2007	181.66	6.80	167.00
5	Iwate_Japan	AKT015	2008	75.75	6.90	244.00
6	Iwate_Japan	AOMH13	2008	159.62	6.90	299.98
7	Iwate_Japan	NIG011	2008	181.93	6.90	185.00
8	Iwate_Japan	YMT015	2008	121.24	6.90	210.00
9	Tottori_Japan	ISK014	2000	289.78	6.61	120.00
10	Niigata_Japan	CHB008	2004	196.41	6.63	205.19
11	Niigata_Japan	CHB015	2004	224.71	6.63	119.98
12	Niigata_Japan	ISK014	2004	240.44	6.63	115.00

Table 3 – Performance levels and performance criteria values

Structure part	Performance criteria	Performance levels and criteria values		
		Immediate occupancy (IO)	Life safety (LS)	Collapse prevention (CP)
Concrete structure	Inter-story drift	1/800	1/300	1/50
Wood substructure	Inter-story drift	1/250	1/100	1/50
Rubber bearing	Displacement	—	—	Min{0.55D,3T_r}

Note: D-diameter of the bearing; T_r-total thickness of the rubber layers

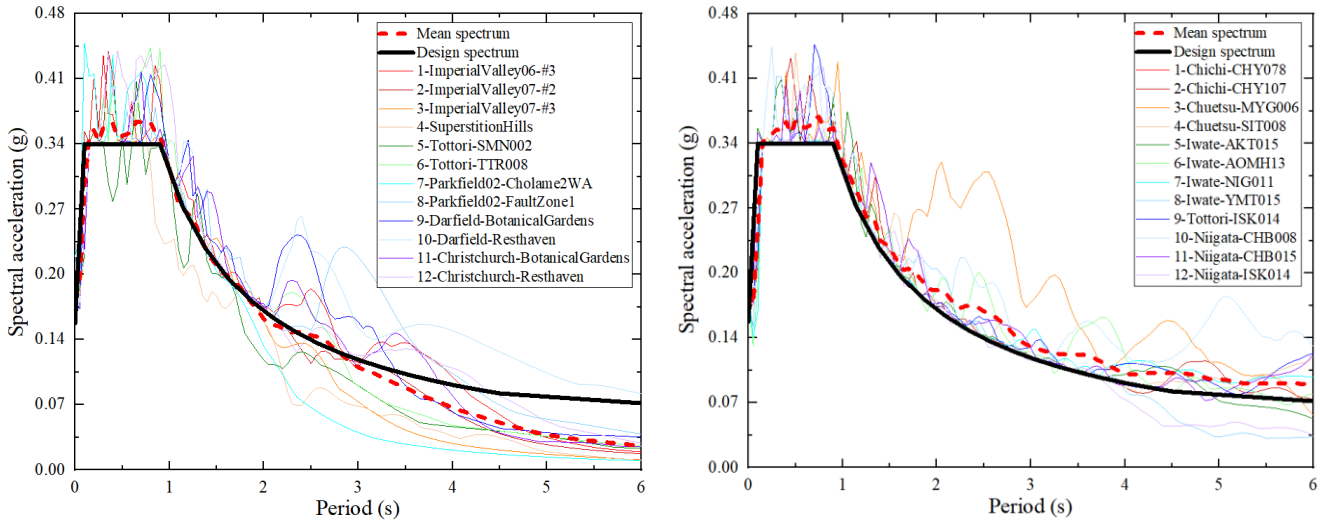

(a) Near-field ground motions (b) Far-field ground motions

Fig.5 – Comparison of the design spectrum and selected ground motions

3. Fragility analysis results

3.1 Seismic response analysis results

Fig.6(a), Fig.7(a), Fig.6(c) and Fig.7(c) show the maximum inter-story drifts of the concrete main structure and wood substructures of the Bolt connection model (BM) under near-field or far-field earthquakes, respectively, while Fig. 6(b), Fig.7(b), Fig.6(d) and Fig.7(d) show those of the Rubber bearing model (RM), respectively. The dash lines in Fig.6 and Fig.7 represent the performance criteria values of IO, LS and CP levels. Fig.8(a) and Fig.8(b) illustrate the maximum displacement of isolation layers under near-field or far-field earthquakes, respectively.

As seen from Fig.6 and Fig.7, with same earthquake levels, the inter-story drifts of the concrete main structure and wood substructures of RM were generally smaller than those of BM, because the isolation layers in RM provided isolation effect to the wood substructures, and also seismic reduction effect to the concrete main structure. Meanwhile, the seismic responses of both concrete main structure and wood substructures under far-field earthquakes were more significant than those under near-field earthquakes. The reason was that the duration of the far-field earthquakes was usually longer, with more long-period frequency parts. The seismic responses of isolation layers were similar under either near-field or far-field earthquakes, as shown in Fig.8.

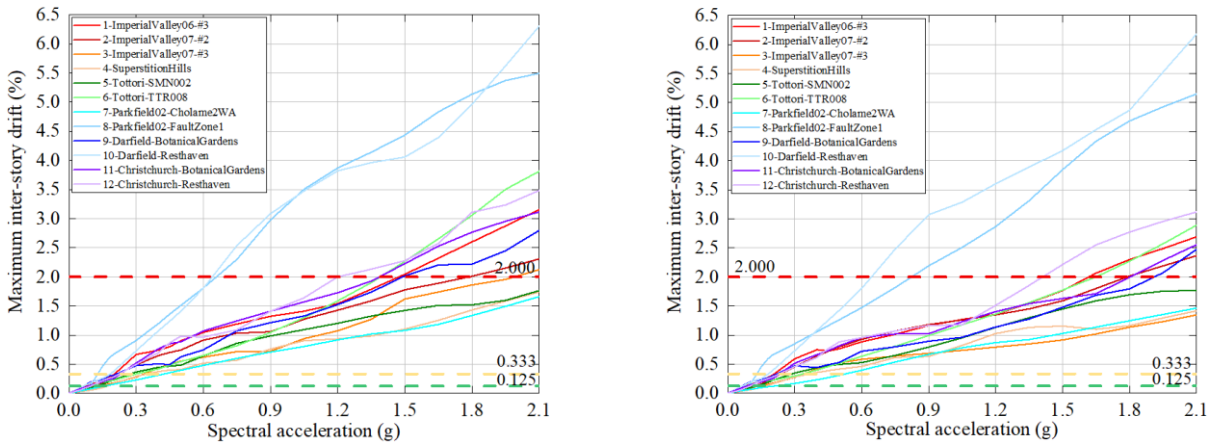

(a) Concrete main structure of BM (b) Concrete main structure of RM

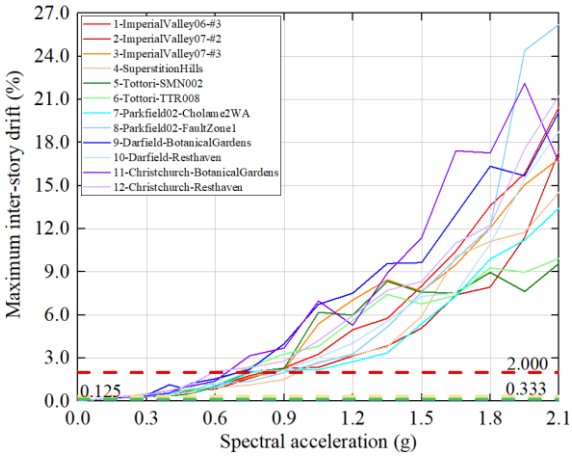

(c) Wood substructure of BM

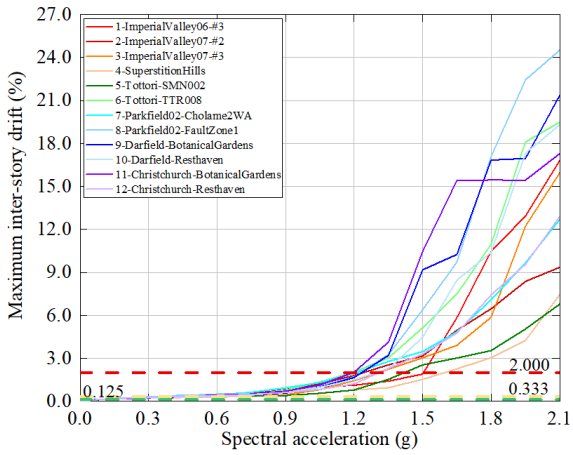

(d) Wood substructure of RM

Fig.6 – Seismic responses of concrete and wood structures in BM and RM under near-field earthquakes

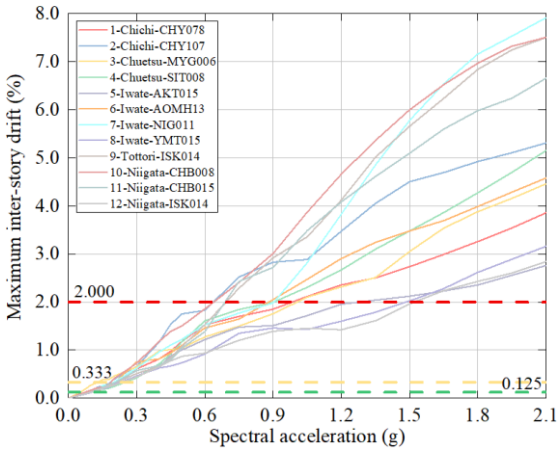

(a) Concrete main structure of BM

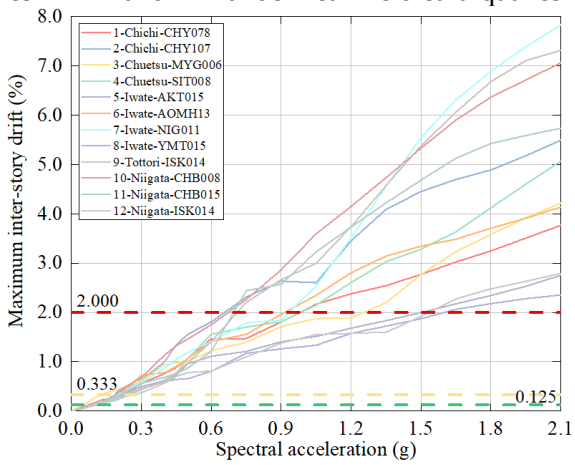

(b) Concrete main structure of RM

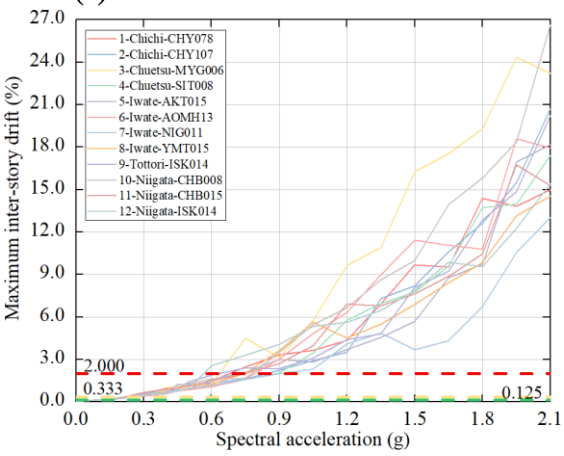

(c) Wood substructure of BM

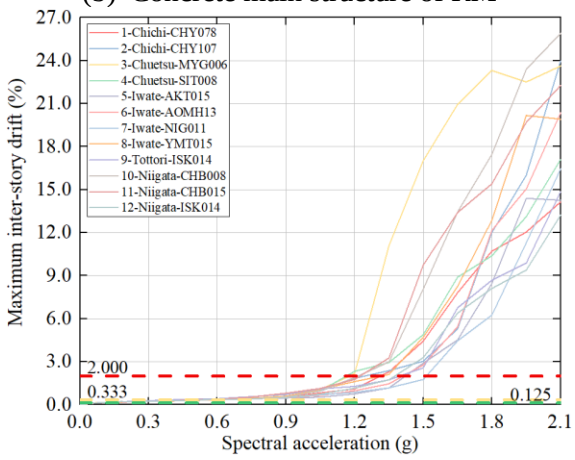

(d) Wood substructure of RM

Fig.7 –Seismic responses of concrete and wood structures in BM and RM under far-field earthquakes

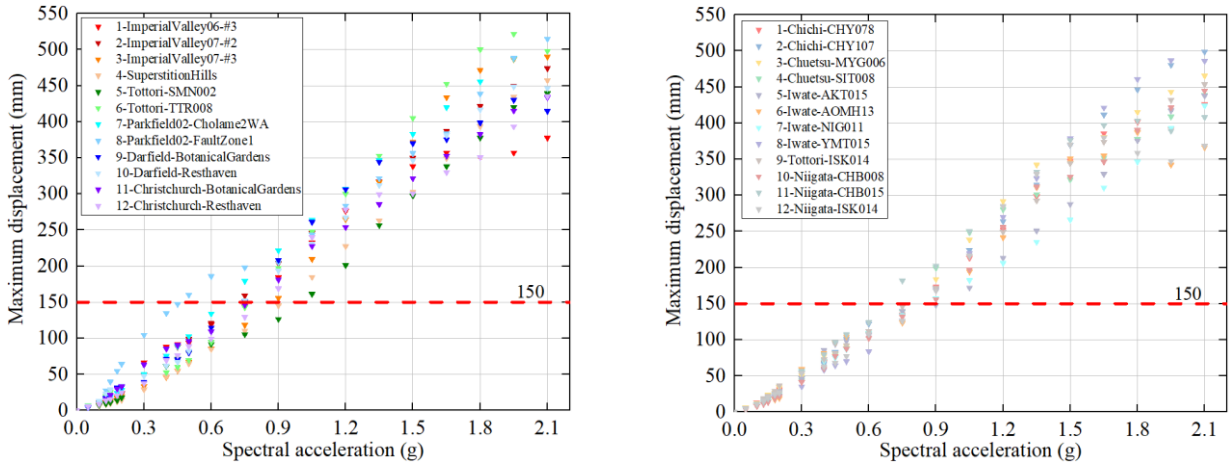

(a) Under near-field earthquakes (b) Under far-field earthquakes

Fig.8 – Seismic responses of isolation layers in BM and RM under near-field and far-field earthquakes

3.2 Fragility analysis results

Fig.9 presents the seismic fragility curves of the concrete main structure and wood substructures under the IO, LS and CP levels and Fig.10 presents the seismic fragility curves of isolation layers under the CP level. The curves tended to be flat as the performance level increased, i.e., the exceedance probabilities (EPs) gradually decreased, which was in accordance with structural design codes.

Comparing the seismic fragility curves of FaB under near-field and far-field earthquakes, it was found that the hybrid system was more sensitive to far-field earthquakes. The EPs of both the concrete structure and wood substructures of BM and the concrete structure of RM under far-field earthquakes were larger than those under near-field earthquakes, while the EPs of the rubber bearing connection and wood substructures with rubber bearings under near-field or far-field earthquakes were similar.

The failure sequence of the hybrid system was reflected by the seismic fragility curves. The results showed that the failure sequence of FaB under both near-field and far-field earthquakes was satisfactory. For BM, the concrete main structure reached the target performance levels ahead of the wood substructures in the IO and LS levels, while in the CP level, the failure probability of concrete main structure was obviously smaller than that of wood substructures, which indicated that the concrete main structure provided the vast majority of lateral resistance and stiffness under earthquakes and would not collapse before wood structures under rare earthquakes. For RM, the sequence of concrete structure and wood substructures were similar in the IO and LS levels, while in the CP level, the isolation layers would firstly achieve the target performance level, then the wood substructures, and finally the concrete main structure, which was in accordance with the design expectations.

Meanwhile, the influence of the connection between the concrete main structure and wood substructures was also demonstrated by the fragility curves. The EP of wood substructures in RM was much smaller than that in BM under all three levels, while for the concrete main structure, the EP of that in RM was evidently smaller than that of BM in the CP level but was similar in the IO and LS levels, under either near-field earthquakes or far-field earthquakes. The results indicated that the rubber bearing connection had a dominant isolation effect on wood substructures and a seismic reduction effect on the concrete main structure.

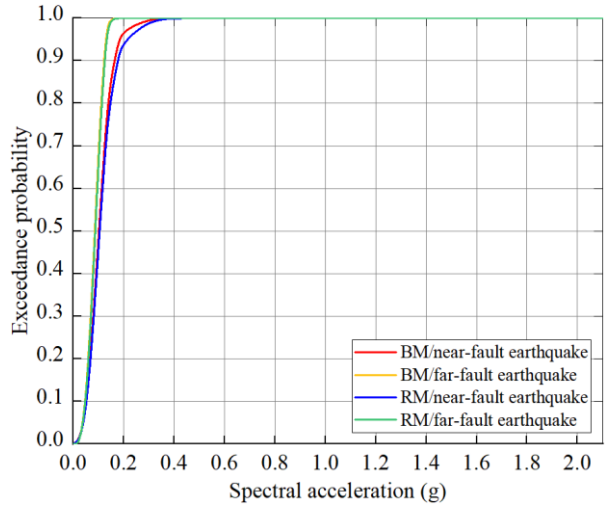

(a) Concrete main structure of IO level

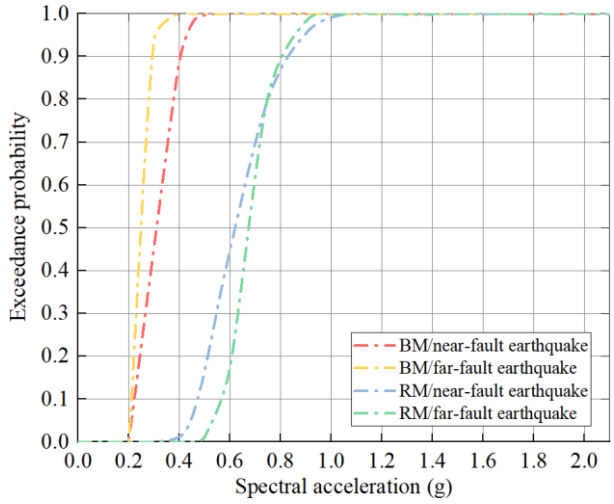

(b) Wood substructures of IO level

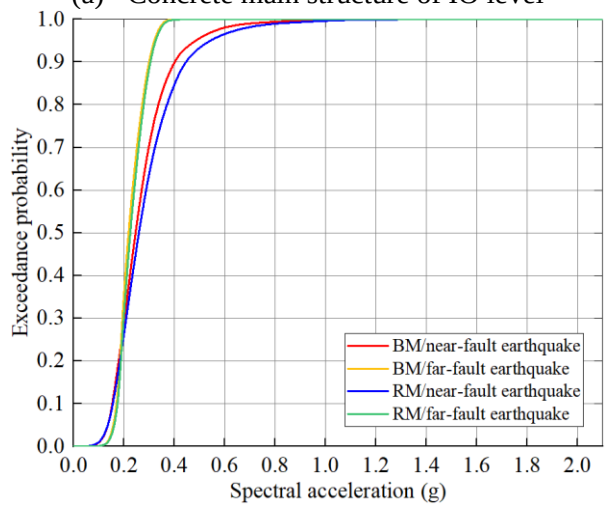

(c) Concrete main structure of LS level

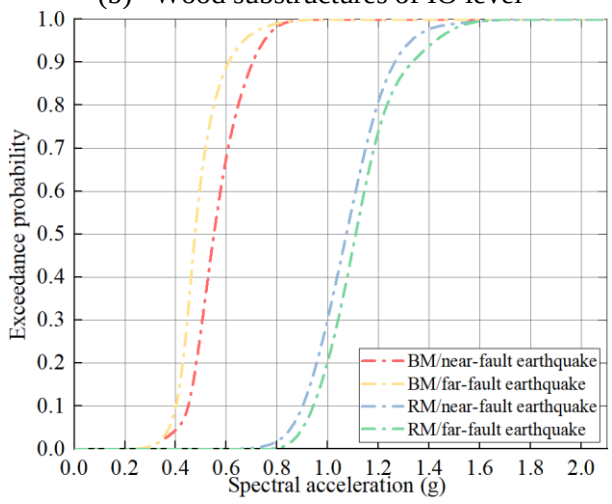

(d) Wood substructures of LS level

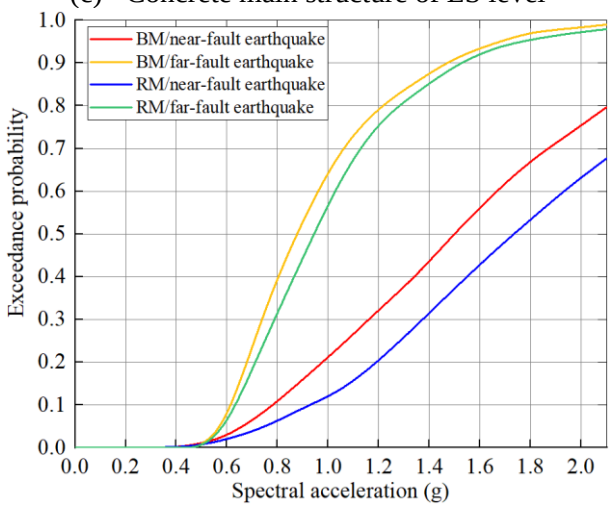

(e) Concrete main structure of CP level

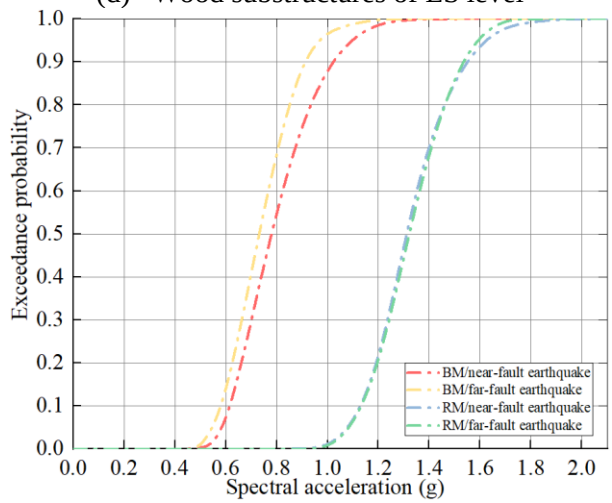

(f) Wood substructures of CP level

Fig.9 – Seismic fragility curves of concrete and wood structures under near-field and far-field earthquakes

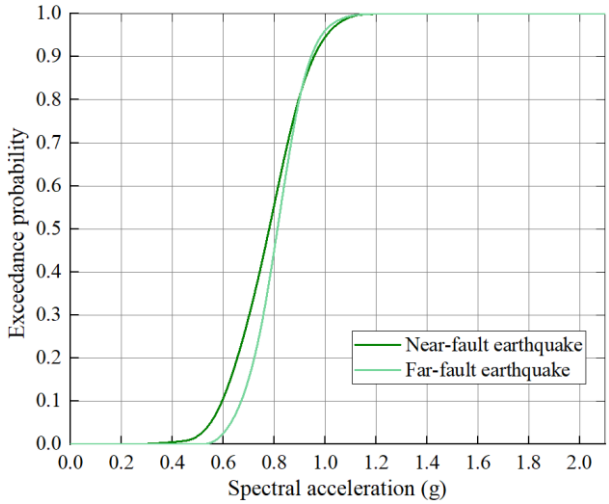

Fig.10 – Seismic fragility curves of isolation layers under near-field and far-field earthquakes

4. Conclusions

The performance-based seismic fragility analysis of a novel concrete-wood hybrid structural system "FaB" was presented. Firstly, the concepts and the numerical finite element models of FaB were introduced. Three seismic performance levels including immediate occupancy (IO) level, life safety (LS) level and collapse prevention (CP) level were then established, and the corresponding performance criteria and values were defined. Based on the incremental dynamic analysis utilizing 12 near-field earthquake motions and 12 far-field motions scaled by the design spectrum with spectral acceleration amplitude from 0.05g to 2.10g, seismic fragility curves of the hybrid system were established by considering different target non-exceedance probabilities. From the results presented in this paper, the following main conclusions can be drawn:

(1) The hybrid system was more sensitive to far-field earthquakes, as the exceedance probabilities (EPs) of the BM and the concrete structure of RM under far-field earthquakes were larger than those under near-field earthquakes, while the EPs of the rubber bearing and wood substructures of RM under near-field or far-field earthquakes were similar.

(2) The failure sequence of FaB under both near-field and far-field earthquakes was satisfactory. In the IO and LS levels, the concrete main structure reached the target performance levels ahead of the wood substructures. In the CP level, the failure probability of concrete structure was much smaller than that of wood substructures in BM, while in RM, the isolation layers would achieve the target performance level first, then the wood substructures, and finally the concrete structure.

(3) The rubber bearing connection had an obvious isolation effect on the wood substructures and a seismic reduction effect on the concrete main structure. The EP of wood substructures in RM was smaller than that in BM under all three levels, while for the concrete main structure, the EP of that in RM was smaller than that of BM in the CP level but was similar in the IO and LS levels.

5. Acknowledgements

The support provided by the National Natural Science Foundation of China (51978502) and the Fundamental Research Funds for the Central Universities (22120180315) is gratefully acknowledged. Special thanks are given to the China Scholarship Council, which supports the second author for the research work in UBC (No. 201906260182).

6. References

[1] Foster RM, Reynolds TP, Ramage MH (2016): Proposal for defining a tall timber building. *Journal of Structural Engineering*, **142** (12), 02516001.
[2] Kuilen JWGVD, Ceccotti A, Xia Z, He M (2011): Very tall wooden buildings with cross laminated timber. *Procedia Engineering*, **14**, 1621–1628.
[3] Izzi M, Casagrande D, Bezzi S, Pasca D, Follesa M, Tomasi R (2018): Seismic behaviour of Cross-Laminated Timber structures: A state-of-the-art review. *Engineering Structures*, **170**, 42–52.
[4] Hristovski V, Dujic B, Stojmanovska M, Mircevska V (2012): Full-scale shaking-table tests of XLam panel systems and numerical verification: Specimen 1. *Journal of Structural Engineering*, **139** (11), 2010–2018.
[5] Cao J, Xiong H, Chen J, Huynh A (2019): Bayesian parameter identification for empirical model of CLT connections. *Construction and Building Materials*, **218**, 254–269.
[6] Tannert T, Moudgil M (2017): Structural design, approval, and monitoring of a UBC tall wood building. *Structures Congress 2017,* American Society of Civil Engineers, Denver, USA, 541–547.
[7] Abrahamsen R (2017): Mjøstårnet - Construction of an 81 m tall timber building. *Internationales Holzbau-Forum IHF 2017* , Garmisch-Partenkirchen, Germany, 1–13.
[8] Xiong H, Ouyang L, Wu Y, Lu S (2016): Preliminary design of a novel hybrid tall building with concrete frame-tube and light wood boxes. *World Conference on Timber Engineering,* WCTE 2016, Vienna, Austria.
[9] Xiong H, Chen J, Wu Y (2018): Research on seismic performance of a concrete-wood hybrid structural system for tall building. *Journal of Building Structures*, **39** (8), 62–70.
[10] Kaushik K, Tannert T (2017): Feasibility study of a novel tall concrete-wood hybrid system. *Structures Congress 2017,* American Society of Civil Engineers, Denver, USA, 411–418.
[11] Chen J, Xiong H, Jiang J (2018): Comparison of two kinds of connections between timber module and concrete structure based on non-linear numerical analysis. *World Conference on Timber Engineering,* WCTE 2018, Seoul, Korea.
[12] Rosowsky DV, Ellingwood BR (2002): Performance-based engineering of wood frame housing: Fragility analysis methodology. *Journal of Structural Engineering*, **128** (1), 32–38.
[13] Kim JH, Rosowsky DV (2005): Fragility analysis for performance-based seismic design of engineered wood shearwalls. *Journal of structural engineering*, **131** (11), 1764–1773.
[14] Li Z, He M, Li M, Lam F (2014): Damage assessment and performance-based seismic design of timber-steel hybrid shear wall systems. *Earthquakes and Structures*, **7** (1), 101–117.
[15] Zhang X, Shahnewaz M, Tannert T (2018): Seismic reliability analysis of a timber steel hybrid system. *Engineering Structures*, **167**, 629–638.
[16] Pan Y, Ventura CE, Finn WL, Xiong H (2019): Effects of ground motion duration on the seismic damage to and collapse capacity of a mid-rise woodframe building. *Engineering Structures*, **197**, 109451.
[17] McKenna F (2011): OpenSees: a framework for earthquake engineering simulation. *Computing in Science & Engineering*, **13** (4), 58–66.
[18] Mattacchione A (1991): Equivalent frame method applied to concrete shearwalls. *Concrete International*, **13** (11), 65–72.
[19] Itani RY, Tuomi RL, McCutcheon WJ (1982): Methodology to evaluate racking resistance of nailed walls. *Forest Products Journal*, **32** (1), 30–36.
[20] Vamvatsikos D, Cornell CA (2002): Incremental dynamic analysis. *Earthquake Engineering & Structural Dynamics*, **31** (3), 491–514.
[21] Chiou B, Darragh R, Gregor N, Silva W (2008): NGA project strong-motion database. *Earthquake Spectra*, **24** (1), 23–44.

